

Application of Modern TSP Technology for Advanced Prediction Prior to Launching TBMs Shiva & Shakti for Up and Down Line Tunnels in the Himalayan Geology of the Rishikesh-Karan Prayag BG Rail Line Project in Uttarakhand, India

Mr. Gajendra Pratap Singh¹, Dr. Prof. Sandeep Potnis² Mr. Rakesh Arora³

¹M-tech Student, Department of Civil - Tunnel Engineering, MIT World Peace University, Pune

²Project Guide, Head of Tunnel Engineering Department, MIT World Peace University, Pune

³ Project Director, L&T, RVNL, Package -4, (RSKH-KNPG) BG Rail line Project, Uttarakhand, India

Abstract-The application of Modern Tunnel Seismic Prediction (TSP) technology in the Rishikesh Karan Prayag new BG rail line project (RSKH-KNPG), particularly in Package-4, has been pivotal in predicting rock mass conditions ahead of the Up and Down line tunnels at both faces. This advanced method has facilitated a comprehensive and accurate study of rock mass behavior, conditions, weak features, projections, weak zones, shear zones, natural caves, and water-bearing strata along the twin tunnel alignments for the safe launching of two Tunnel Boring Machines (TBMs) named Shiva and Shakti. M/s L&T /RVNL implemented the TSP investigation at two strategic locations inside the large semi-underground railway station junction for the Up and Down line tunnels.

The necessity to evaluate TSP's efficacy in assessing geo-hydrological conditions, bonding, rupturing, and other geological features prompted a comparison with other investigation methods used within 100 meters from both tunnel faces (CH: 48+180m and RD857m). TSP method results were compared with engineering geological predictions and estimated geological cross-sections, revealing that TSP effectively detects varying rock mass zones in the Himalayan geology. However there was no direct relationship in between wave velocities (V_p and V_s) and the Q & RMR values, a linear regression analysis highlighted the potential of TSP in identifying hard, medium, and soft weak zones of rock mass.

Additionally, comparisons with Measurement While Drilling (MWD) results indicated that TSP and MWD could complement each other, identifying weak zones where one method might not detect them. The complex geology of Package-4, with its varying rock mass quality (RMR ranges 39-49 and 36-43 for the Up and Down line tunnels, respectively), suggests that TSP technology is

well-suited for such challenging geological conditions. The findings underscore the importance of incorporating TSP for ensuring safety and precision in tunnel boring operations in the Himalayan region.

Keywords: Tunnelling, rock mechanics, RMR, engineering geology, TSP, Ground Parameters, TBM - tunneling, NATM, Geotechnical Assessment, Junction, refraction, cavity shear, water bearing, strata zones.

INTRODUCTION

The Rishikesh-Karanprayag new BG rail line project (RSKH-KNPG) is a significant development initiative undertaken by the Ministry of Railways. The project aims to establish rail connectivity between Rishikesh and Karnaprayag, facilitate easy access to pilgrimage sites in Uttarakhand, connect new business hubs, develop backward areas and serve the local population. The total length of the rail line is 125 km, divided into nine construction packages. This ambitious project includes 17 tunnels with a total tunneling length of 105 km, meaning approximately 84% of the alignment will pass through tunnels.

It is important to Characterize the rock mass condition before the tunnel face to identify weak zones, fault and shear seams, cavities, and water-bearing geological structures in a cost-effective manner for Package-4, TSP measurements to provide these insights was planned. This package consists of

Tunnel T8, featuring parallel Upline (M/T) and Downline twin tunnels with finished lined diameters of 7.8meters. The construction of Package-4 is being executed in two parts. The first part, from CH48+180 to CH58+730, is being excavated using Tunnel Boring Machines (TBMs). The second part, from CH58+730 to CH62+165, is under construction using drilling and blasting with the New Austrian Tunneling Method (NATM). Additionally, construction from P2 is progressing using drilling and blasting with NATM methods through a circular vertical shaft at CH62+680.

The TSP campaign was conducted for both the Upline and Downline tunnels, where two TBMs (Shiva and Shakti) were launched. At the time of the TSP measurement, the tunnel face positions was at CH48+180 for the Upline tunnel and RD857 for the Downline tunnel. Prior to launching the TBMs from the nearby underground double-track railway station junction, modern TSP303 Plus technology was employed to predict the geological conditions in both tunnel alignments within the Himalayan geology.

The progress of the Upline (M/T) and Downline tunnels from Portal (P1) has reached approximately 75%, driven by the twin TBMs, Shiva and Shakti. The project continues to advance, demonstrating the effectiveness of integrating modern TSP technology into tunneling operations in complex geological settings. This thesis explores the application of TSP technology in Package-4, highlighting its role in ensuring safe and efficient tunneling in the challenging Himalayan geology.

1.0 PROJECT GEOLOGICAL FORMATION:

The Garhwal region of Western the Himalaya, located between the Kali River in the east and Sutlej in the west, covers 320 km of terrain. The Lesser Himalaya comprise a thrust - bound sector delineated by two tectonic plates - the Main Boundary Fault in the south and the Main Central Thrust to the north. This area is entirely belonging to low grade metamorphic rocks of Chandpur formation of Jaunsar Group. The rock mass is continuous sequence of light and dark grey phyllite as well as light grey and purple sandstone and siltstone. The quartz schist is also noticed in thin band with phyllite. These exhibit remarkably uniform lithology and outcrops widely

between Kolta and Rampur villages. From Ch. 58+730km to Janasu village 62+580km (left bank of Alaknanda River), the direction of schistosity is almost NNW-ESE (T8), plunging NE and SW due to the presence of chevron folds, with axis-oriented ESE-WNW. The ESE-WNW- system is clearly more evident approaching to the North Almora Thrust (NAT). Minor Low angle thrust fault zones have been observed inside the Phyllite sequence. NE dipping thrust planes were observed with typical movement indicators. In the railways tunnel -8 alignment phyllite rock mass is recorded.

1.1 U/P line tunnel site geology between CH; 48+148 to 48+180 during TSP Tests.

In the MT-TBM LAUNCHING DOWN LINE U/L (heading) excavation, the given stretch of the tunnel found to consist of grey colored, moderately strong, highly jointed, slightly weathered Quarzitic phyllite. At present 3 sets of prominent joints were observed at the face having very low to medium persistence. The joints are mostly close spaced having partly open to open aperture. Quartz and silty clay infilling were also observed along the joints. The joint surfaces are slightly rough to smooth at places. 5 to 10cm thick shear observed at crown and face. Dampness observed along the shear (RMR 36 - 43). Average Overburden cover in the tunnel alignment at TSP campaign location 260 m. TSP campaign conducted at Ch 48+180 in MT-TBM launching tunnel U/L. During this campaign 24 drill holes of 1.5m long for blasting are done between Ch 48+148 to 48+180. This campaign predicted prediction of ground conditions from CH- 48+180 to 48+290 (total 110m) and for good results considered for TSP layout (Ch 48+ 180 – 48+ 119) as per site conditioned. (Ref – Fig-1),

1.2 D/N line tunnel site geology between CH; 821.50 to 877.866m during TSP Tests.

In the TBM LAUNCHING DOWN LINE (Heading) excavation, this stretch of the tunnel is found to consist of greenish grey, light grey colored and grey colored, moderately strong, moderately jointed, slightly weathered Quarzitic phyllite. At present 3 sets of prominent joints were observed at the face having very low to medium persistence. The joints are mostly close spaced having partly open to open aperture. Quartz and silty clay infilling were also

observed along joints. The joint surfaces are slightly rough to smooth at places. Multiple Shearing (50-100mm) observed on the tunnel face. Warping along the joints was also observed on the current tunnel face. (RMR- 39- 44) TSP campaign conducted at Ch 857.5 in MT-TBM launching tunnel D/L. During this campaign 24 drill holes of 1.5m long for blasting are done between Ch 821to 857.5.This campaign predicted prediction of ground conditions from CH-857.5 to 996 (total 137m). (Ref-Fig1)

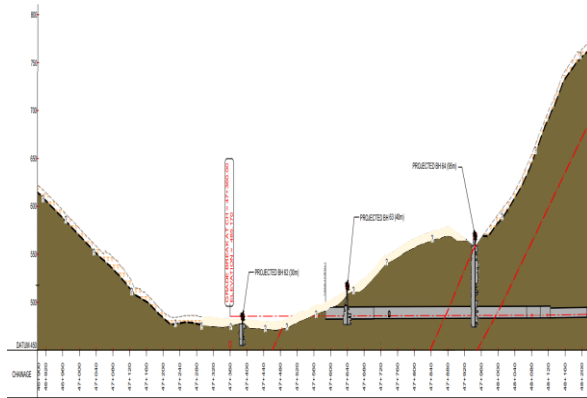


Fig-1 TSP campaign locations on geological section of Tunnel T8

2. TSP METHODS

2.1 Principal concept

Principal of TSP detects changes in rock mass such as irregular bodies, Discontinuities, fault and fracture, weak zones , shear zones , water holding level of strata, tunnel front areas. Employed as a predictive method during excavation process for both drill & blast and TBM launching headings, the measurements do not require access to the face , which were taken in tunnel production breaks of approximately 60 minutes. Acoustic signals are typically generated by a series of 24 shots of 50 to 100 grams of detonation cord aligned along one tunnel wall and and in cases of more complex geology and additional shot line along the opposite tunnel wall. Four sensor probes, equipped with highly sensitive tri-axis receivers, are contained in safety tubes whose tips are firmly cemented into 45-50 mm boreholes in both sidewalls (Figure 2). 3-component receivers capture the seismic signals, which were then reflected off any kind of discontinuities in the rock mass. A highly sophisticated processing and

evaluation software was designed for ease of operation. The system’s ability to record full wave field of compression and shear waves in combination with intelligent analysis software enables the determination of rock mechanical properties such as Poisson’s ratio and Young’s Modulus within the prediction zone. The final 2D- & 3D-summary results generated by the system software represent well detected events and boundary planes crossing the tunnel drive axis along the face coordinates.



Figure 2. Standard TSP measuring layout with 24 explosive charges are being shot one by one with closed to tunnel drive face on right or left tunnel walls. Four receivers arranged further back pick up arriving waves.

2.2 Carried out Operation.

The system installation and setup with four sensitive tri-axis sensors is simple and comparable to installing rock bolts, taking a total of 45 minutes. In such system seismic acquisition geometry is limited to the source and receiver at or near the tunnel. As a result, the reflection and scattering angles are small and spatial resolution is not optimal when imaging forward obstacles. Seismic problems are further decreased by seismic waves, which require high frequencies, which are remarkably strong. Therefore, it is very important to document data to avoid incorrect seismic predictions ahead of tunnel, which may be lead to incorrect specifications. For example, discontinuities, fracture, weak, soft areas which are structural or geological features that alter the uniformity in the rock mass, can not be imaged at full scale, as only narrower portions of these areas are transmitted to the receiver side of the wave , can reflect the physical Snell’s law of reflection. The

image would be enhanced by using more receivers, such as two on either side of both tunnel wall sides. Furthermore, when the rock mass is very complex in terms of alternative strike angles or irregular obstructions such as cavities or Karst features, it may be quite worthwhile to provide a second source line along the opposite tunnel wall. By all means, any increase in the amount of acquisition data produces higher quality result images, especially when it comes to 3-D data processing.



Figure 3 (i). Installation of receivers and recording unit to TSP campaign.

The TSP 303 system integrates 3D data acquisition and processing software that includes routines for optimal seismic imaging in relation to tunneling requirements. It uses information in the seismic wave field by discrete compression (P) and shear (S) wave analysis and 3D-velocity based migration and reflector extraction techniques (3D-VMR). 3DVMR technology provides adequate and detailed 3D images of the ground leading to more reliable interpretation than traditional 2D approaches.



Figure 3-(ii) Simple installation, process for receiver recording & unit with system (TSP 303 Plus).

2.3. Wave velocity and related parameters

Elastic body waves passing through homogeneous, isotropic media have well-defined equations of motion. Using these equations, the geo-mechanical properties of a rock mass can be calculated. Field surveys like the TSP method can easily obtain wave velocity, V_p and V_s ; Velocities are in units of length per time, usually meters/second (m/s). Engineering properties of a homogeneous, isotropic medium such as: Young's or elastic modulus (E), shear modulus (G) and Poisson's ratio can be determined if V_p and V_s are known with accounting for representative density values.

$$\sigma = \frac{1}{2} (V_p^2 - 2V_s^2) / (V_p^2 - V_s^2) \text{ Poisson's ratio}$$

$$E = \rho V_p^2 (1-2\nu)(1+\nu)/(1-\nu) \text{ Young's or elastic modulus}$$

$$G = E/[2(1+\nu)] \text{ Shear modulus}$$

2.4 Limitations conditional upon geology

Appropriate rock physical property contrasts will exist along fault zones or changes in rock mass formation. Seismic applications employ the parameter of acoustic impedance (the products of body wave velocity and rock density) that is a measure of quality determining the reflection coefficient. An acoustic impedance contrast of at least 20% ensures sufficient strong reflection signals to seismically detect geological discontinuities.

The general TSP® layout works most accurately for rock boundary orientations that intersect the tunnel drive axis at a moderate to high angles. Thus, a certain strike and dip angle ($>25^\circ$) with respect to the tunnel drive direction can be predicted by TSP®. Best results are being achieved at steeply dipping or striking boundaries ($>45^\circ$). Boundaries ahead of the tunnel face showing lower angles ($<25^\circ$) aren't able to reflect signals to the receivers due to the receivers' back arrangement of approx. 50 m behind the tunnel face. This restriction belongs to physical Snell's law.

Standard TSP data processing and modelling had been developed for data acquired in tunnels with high overburden (>50 m). Although not restricted, results analysis and interpretation can be carefully done for tunnel with lower overburden (<50 m) considering result extrapolation beyond the actual surface.

3. OPERATIONAL COMMENTARY

3.1 Site Preparation and Measurements

Total 24 shot holes and 4 receiver holes were drilled for each campaign based According to standard TSP layout, opposite receiver’s hole position was falling in the unction of upline & downline tunnel, where distance between both tunnel wall was ~ 2m. To avoid the impact tunnel geometry on seismic signal, it was decided to keep all 4 receivers on left tunnel wall as shown in Figure 2. The shot holes were drilled on left side of tunnel wall for Up Line tunnel. And as per standard procedure, the shot and receiver boreholes of the TSP layout along the tunnel walls were checked upon correctness of length, diameter, alignment and access. After about 30 minutes of clearing up the boreholes & installation of sensor, setup activities of the TSP 303 Plus system started by TSP Operators.

Simultaneous to the system installation, the explosive charge preparation was also shortly explained to the blaster team. It had been agreed on the use of electric delay detonators. The use of delayed detonators implies the use of the Wire Break Trigger mode (WBT) of the TSP 303 Recording Unit as shown in 4. The WBT mode allows the use of delay detonators despite the request for very high accuracy of the trigger time of each shot. To check the optimum charge size, the first shot point (SH-1) was charged with 50 g of explosive and sandbags were used for stemming, which generated magnitude of 336 mV, which is above the minimum recommended signal amplitude (100 mV). The charge size was increased stepwise towards face and their details are given in Table 1,2,3&4 for Up and down line tunnels.



Figure 4 Detonator cap with wrapped round wire (white) that gives the accurate recording trigger in the moment of blast (WBT-mode).

Table 1 - Details of charge size (Up line tunnel)

Shot hole	Charge size (gram)
1-4	50
5-10	80
11-13	100
14-17	130
18-20	180
21-24	250

Table 2 - Details of charge size (Up line tunnel)

Shot hole No	Charge size (grams)	Recording time (Inclusive loading & recording)
1 - 4	50	17:43 – 19:52 (2 hr 20 minutes approximately)
5 - 9	80	
10 - 15	130	
16 - 24	195	

Table 3 Specification of TSP layout during recording for Up line (U/L) tunnel

Campaign Name		TBM Launching tunnel -Upline
Data Recording date		01 Nov 2022
Measurement in direction of advance		
Shot holes	No. drilled	24
	Diameter	45 mm
	Depth / Location	1.0 m to 1.8 m / along left wall
	Inclination from horizontal	2 to 10.8° downwards
	Spacing	1.2 – 1.7m
	Performed shots	23
	Explosive charges	50 - 250 g (stepwise increasing towards face)
Receiver holes	Number	4
	Diameter	51 mm
	Depth / Location	RCV1 & RCV2 – 1.45/1.72 (right) RCV3 & RCV4 – 1.85/1.79 m (right)
	Inclination from horizontal	8° - 10° Upward
	Nearest offset to first shot hole	13.7 m
	Distance between receiver holes	5 (right) & 5 (right)
Seismic Source		
Blasting machine	Electric Blasting Machine	
Detonators	Delay electronic detonators	
Explosive Type	Indo-super power 390	
Min Detonation Velocity	3500 m/sec	
Type of Triggering	WBT	

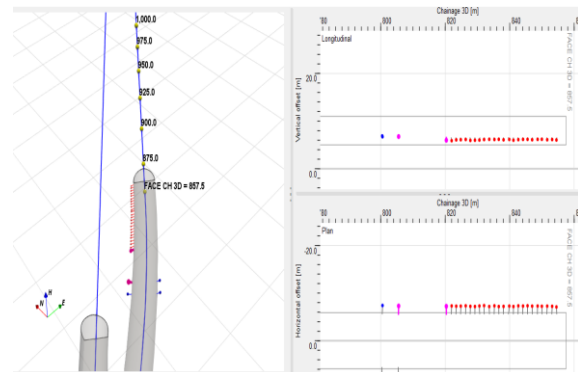


Figure 5 : U/L Actual TSP layout of campaign at upline tunnel at Ch48+180.

Table 4- Specification of TSP layout during recording for D/N line tunnel

Campaign Name	RD857.5_Downline
Data Recording date	08 Nov 2022
Measurement in direction of advance	
Shot holes	No. drilled 24 Diameter 51 mm Depth / Location 1.5 m to 1.8 m / along left wall Inclination from horizontal 11° to 20° downwards Spacing 1.37 – 1.6 m Performed shots 24 Explosive charges 50 - 195 g (stepwise increasing twds face)
Receiver holes	Number 4 Diameter 51 mm Depth / Location RCV1 & RCV2 – 1.7/1.8 (left) RCV3 & RCV4 – 1.52/1.75 m (right) Inclination from horizontal 8.5 - 7° (left) and 12 - 12.5° (right) Nearest offset to first shot hole 14.85 m Distance between receiver holes 5.0 m (left) and 5.15 m (right)
Seismic Source	
Blasting machine	Electronic Blasting Machine
Detonators	delay electronic detonators
Explosive Type	Indo Superpower 90
Min Detonation Velocity	3500 m/s
Type of Triggering	WBT

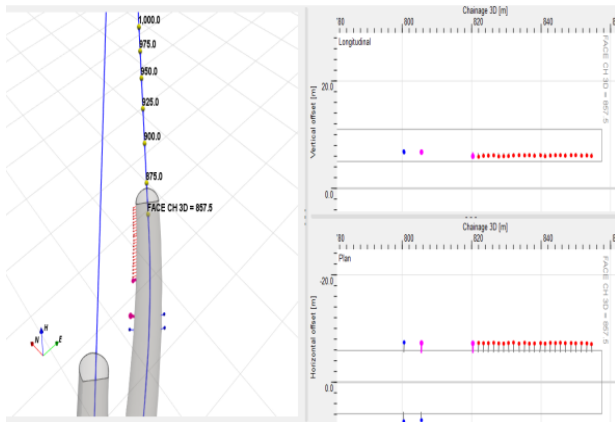


Figure -6 -D/N line tunnel Depicts the seismic layout reproduced in the AMBERG TSP Ease software. The tunnel model exactly resembles the real geometry of the tunnel.



Figure 6: Progressive photographs during TSP operation.

4.0 Result of TSP Campaign – Upline,
4.1.1. 3D Velocity Models, P wave Velocity Model:

Figure-7, depicts 2D longitudinal and plan sections (top and bottom, respectively) extracted. from the 3D model of the P-wave velocity (V_p) on the seismic drive axis. Varying colouring indicates velocity variation, in which blue and red areas correspond to increasing and decreasing wave. velocity, respectively. The description of the velocities & estimated parameters is given in Table 5.

Table 5: 3D model description and features

2D sections						
Model start (Ch): 48,117			Model end (Ch): 48,317, Tunnel face at the time of recording (Ch): 48,180			
V_p (m / s)			V_s (m / s)			
Min.	Ref.	Max.	Min.	Ref.	Max.	comment
3,864	4,093	4,607	2,159	2,366	2,527	<ul style="list-style-type: none"> Reference velocity along the TSP layout Ahead of face velocity slight variation in the velocities has been observed.
Identified Low Velocity Zones (LVZ) *						
Zone	Ch	V_p (m / s)	Location	comment		
I	Approx. 48,229 – 48,243	4,009 – 4,069	Reflector are found from left tunnel wall side.	<ul style="list-style-type: none"> This decrease in V_p may be associated with increase in rock mass fracturing/jointing 		
II	Approx. 48,257 – 48,268	4,018	Cutting the tunnel axis. In this zone, drop in V_s also found where reflectors are mapped from right side.	<ul style="list-style-type: none"> This decrease in V_p may be associated with decrease in rock stiffness 		
* LVZs are commonly associated with changes in rock properties. These changes may be due to increased fracturing or jointing, the appearance of shear zones.						
* Identified LVZs are marked in figure 6.						

Varying coloring in Figure indicates velocity variation in which blue and red areas correspond to increasing and decreasing P-wave velocity. As per velocity distribution, the entire predicted area seems to be almost similar rock mass condition as found in the layout area, however some local improvement in the velocity has been observed except two comparatively low velocity zones, which may encounter tunnel axis approximately CH48,229 and CH48,257 respectively.

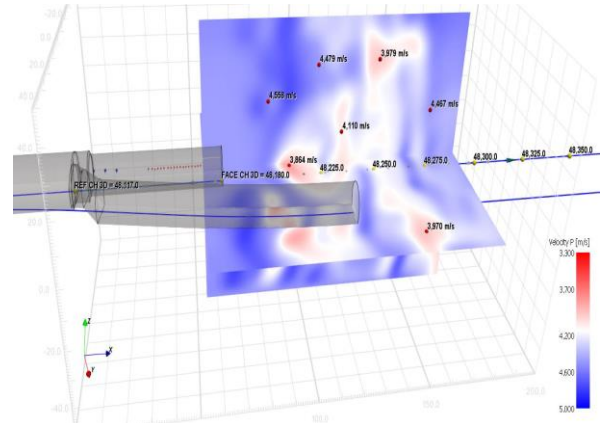


Figure 7: Top & Longitudinal 3D view velocity of P-wave model drive direction with tunnel, including tunnel

model along location of shot holes (red dots), receivers (blue dots). The red dot markings indicate values of V_p at the selected position and Roman numerals indicate relevant comparatively LVZs. (U/L- Line)

4.1.2. S- wave Velocity Model:

Figure 8. Shows 2D longitudinal and plan sections (top and bottom, respectively) that were extracted from the 3D model of S-wave velocity (VS) on the seismic axis.

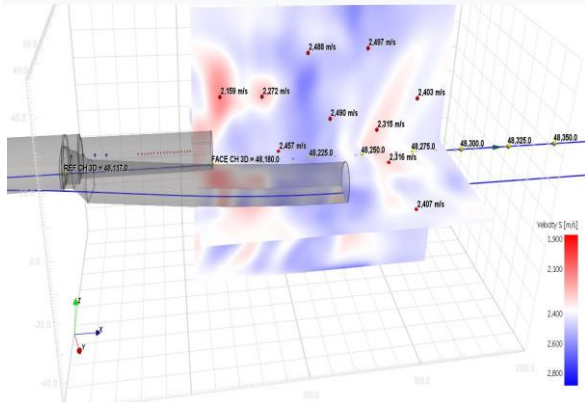


Figure 8- Top & Longitudinal view for 3D S-wave velocity model along tunnel axis including model with location of the shot holes (red dots) and the receivers (blue dots). The comparatively low velocities zones are indicated by black arrows. The red dot markings indicate values of V_s at the selected position (U/L- Line)

A slight decrease in velocity is found directly ahead of tunnel face, which may be associated with increase in rock fracturing or possibly due to blasting impact from surrounding downline tunnel. A 2nd drop in V_s is found approximately from CH48,250 which also correlate with V_p model. The low velocity zones in S wave may be associated with a detriment of the rock condition as will be discussed later in this report.

4.1.3. P- wave Migration:

The process of migration maps seismic amplitude that are recorded as function of time to model space utilizing travel time of waves propagating through the velocity model. Results coming from the 3D processing are represented by two main outputs, the RMS amplitude, and P&S-wave velocity distributions. RMS amplitude distribution quantifies the level of reflectivity throughout the modelled area. Large RMS values with positive or negative signs, correspond to areas of high “illumination”. In other

words, the areas from where the most reflections obtained through 3D processing. This is an output from the so-called seismic migration process. The reflective zones can be associated to boundaries, where significant changes in the rock condition might be expected. Highest negative values (dark blue) are found within the rz1 and rz2. Negative values are associated to changes from higher to low velocity while red values to the contrary.

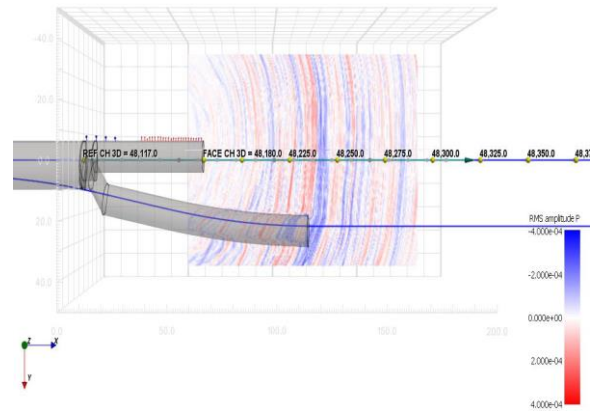


Figure -9 Plan View extracted from the 3D RMS amplitude image for P-wave. High reflectivity zones are shown by black arrow mark U/LLine)

4.1.4. Prognosis along tunnel axis:

The fundamental of the interpretation based on the TSP results relies on the contrast between the reference values, i.e. seismic velocities and geomechanically parameters estimated within the TSP layout and the values of these parameters associated to the reflectors extracted along the prediction ranges allow for an initial correlation of these values for geological observations with drive TSP layout and exiting geological model. Considering these aspects, the prognosis for this campaign is further explained as follows:

Ch 48 + 117m to 48 + 180m (Reference values)

This section corresponds to the TSP seismic layout where a single reference value for each parameter is estimated based on the velocity of the direct waves and an empirical density formula selected from the rock catalogue included in the software AMBERG TSP 303 Plus Ease for the most predominant type of rock along the TSP layout. The estimated parameters along TSP layout of previous & current campaign are given in Table 6. (Table 6: Reference values & estimated parameters)

Table -6

Parameter	#1_Upline - Ch 48,180
Vp (m / s)	4,093
Vs (m / s)	2,366
Poisson ratio (-)	0.25
Edyn (GPa)	34
Stat Edyn (GPa)	18
Geology	Phyllitic quartzite, B3 Class. Ground water condition is dry

a) Ch 48,180 to Ch 48,193

Parameter	Vp [m / s]	Vs [m / s]	Poisson	Edyn [GPa]	Stat Edyn [GPa]
values	4,469	2,311	0.32	35	18
tendency	Increasing	Slight decrease	Increasing	Comparable to ref	Comparable to ref

Interpretation Continuation of almost similar rock mass condition / B3

Remarks Due to decrease in Vs, slight increase in rock mass fracturing/jointing might be expected around the face. This drop in Vs might be associated with blasting impact from downline tunnel.

b) Ch48,193 to CH48,202

Parameter	Vp [m / s]	Vs [m / s]	Poisson	Edyn [GPa]	Stat Edyn [GPa]
values	4,560	2,462	0.29	39	23
tendency	Slight Increase	Increasing	Increasing	Slight decrease	Slight decrease

Interpretation Increase in rock mass stiffness / B3.

Remarks

h) Ch48,265 to Ch48,272

Parameter	Vp [m / s]	Vs [m / s]	Poisson	Edyn [GPa]	Stat Edyn [GPa]
values	4,018	2,428	0.21	35	19
tendency	decreasing	Slight increasing	decreasing	Slight increase	Slight increase

Interpretation Comparatively increase in rock stiffness from previous section.

Remarks

i) Ch48,272 to Ch48,290

Parameter	Vp [m / s]	Vs [m / s]	Poisson	Edyn [GPa]	Stat Edyn [GPa]
values	4,156 - 4,267	2,328 - 2,448	0.24 - 0.29	35 - 37	18 - 20
tendency	decreasing	Slight increasing	decreasing	Slight increase	Slight increase

Interpretation Comparatively increase in rock stiffness from previous section.

Remarks

c) Ch48,202 to Ch48,209

Parameter	Vp [m / s]	Vs [m / s]	Poisson	Edyn [GPa]	Stat Edyn [GPa]
values	4,461	2,285	0.32	34	18
tendency	Slight decrease	decreasing	Slight increase	Slight decrease	Slight decrease

Interpretation Comparatively slight decrease in rock mass stiffness / B3.

Remarks

d) Ch48,209 to Ch48,229

Parameter	Vp [m / s]	Vs [m / s]	Poisson	Edyn [GPa]	Stat Edyn [GPa]
values	4,517 - 4,549	2,345 - 2,440	0.29 - 0.32	36 - 39	20 - 22
tendency	Increasing	Increasing	Slight decrease	Slight increase	Slight increase

Interpretation Slight increase in rock mass stiffness.

Remarks

e) Ch48,229 to Ch48,245

Parameter	Vp [m / s]	Vs [m / s]	Poisson	Edyn [GPa]	Stat Edyn [GPa]
values	4,009 - 4,147	2,412 - 2,434	0.21 - 0.24	35 - 38	19 - 20
tendency	Decreasing	Comparable	decreasing	Increasing	slight increase

Interpretation Slight decrease in rock stiffness / increase in rock mass fracturing might be expected. Lowest values are found from CH48,229 - CH48,235.

Remarks

f) Ch48,245 to Ch48,257

Parameter	Vp [m / s]	Vs [m / s]	Poisson	Edyn [GPa]	Stat Edyn [GPa]
values	4,259 - 4,269	2,417 - 2,419	0.28	38	20
tendency	Slight increase	Comparable	Comparable	Comparable	Comparable

Interpretation Slight increase in rock stiffness.

Remarks

g) Ch48,257 to Ch48,265

Parameter	Vp [m / s]	Vs [m / s]	Poisson	Edyn [GPa]	Stat Edyn [GPa]
values	4,190	2,332	0.28	34	18
tendency	Slight decrease	decreasing	Slight increase	Slight decrease	Slight decrease

Interpretation Slight decrease in rock stiffness / possibly due to increase in fracturing or shear seams.

Remarks In 3D VP & Vs model, a consistent drop in velocity has been observed approximately from CH48,250.

5.RESULT OF TSP CAMPAIGN – DOWN LINE - TUNNEL

5.1.1. 3D Velocity Models, P wave Velocity Model:

Figure 10 shows 2D longitudinal and plan sections (top and bottom, respectively) extracted from the 3D model of the velocity waveform for (P) and (Vp) on the seismic drive axis. Different colors indicate velocity variations, with blue and red areas corresponding to increasing and decreasing P-wave velocity, respectively. Details of velocity and estimated parameters are given in Table 7.

Table -7 : 3-D model description and features

2D sections						
Model start (RD): 798			Model end (RD): 998, Tunnel face at the time of recording (RD): 857			
Vp (m / s)			Vs (m / s)			
Min.	Ref.	Max.	Min.	Ref.	Max.	comment
4,148	4,936	5,419	2,494	2,853	3,057	<ul style="list-style-type: none"> Reference velocity along the TSP layout Ahead of face velocity slight variation in the velocities has been observed.
Identified Low Velocity Zones (LVZ) *						
2D sections						
Model start (RD): 798			Model end (RD): 998, Tunnel face at the time of recording (RD): 857			
Vp (m / s)			Vs (m / s)			
Min.	Ref.	Max.	Min.	Ref.	Max.	comment
4,148	4,936	5,419	2,494	2,853	3,057	<ul style="list-style-type: none"> Reference velocity along the TSP layout Ahead of face velocity slight variation in the velocities has been observed.
Identified Low Velocity Zones (LVZ) *						
Zone	RD	Vp (m / s)	Location	comment		
I	Approx. 867 – 892	4,148-4,669	Reflectors are mapped from right tunnel wall side, where dropped to 4,092m/s.	<ul style="list-style-type: none"> This decrease in Vp may be associated with decrease in rock stiffness 		
II	Approx. 907 – 913	4,728	Reflectors are mapped from right tunnel wall side, where dropped to 4,229m/s.	<ul style="list-style-type: none"> This decrease in Vp may be associated with slight decrease in rock stiffness 		

* LVZs are commonly associated with changes in rock properties. These changes may be due to increased fracturing or jointing or shear zones.

Varying coloring in Figure 10 indicates velocity variation in which blue and red areas correspond to increasing and decreasing P-wave velocity. As per velocity distribution, the entire predicted area has increasing trend in velocities except two sections where Vp dropped below the reference value. As shown in figure10, lower value is measured towards right tunnel wall side and their details are given in Table 7. Figure 11 shows the identified low velocity zones of compressional wave with a render value. Vp=4,500 m/s. Geological features like anomalous velocities can be visualized in 3D using the surface rendering feature of TSP interpretation software. As shown in Figure 11, 1st anomalous zone found close to face (~10m from axis, towards right wall), however the 2nd is found slightly away from tunnel axis (~20-25m from axis, towards right wall).

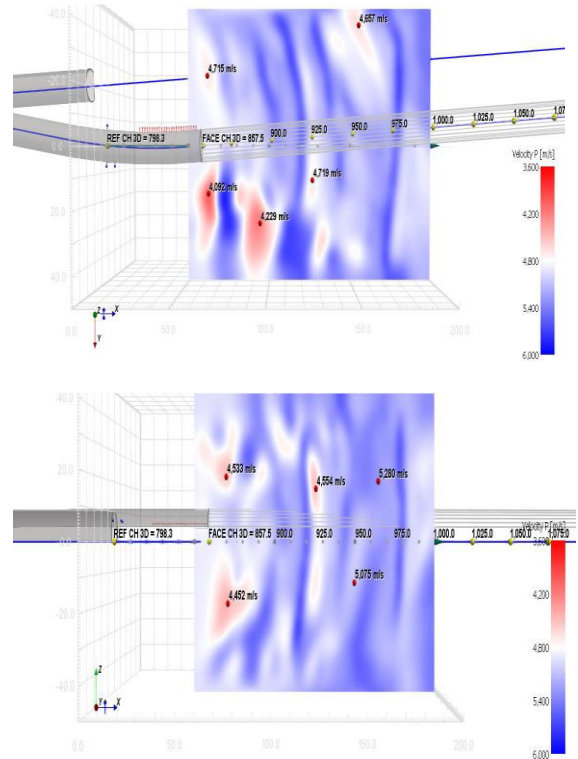


Figure 10 :Top & Longitudinal for 3D- view for P-waves velocities model in tunnel drive axis including the tunnel model, location of shot holes (red dots) and the receivers (blue dots). The red dot markings indicate values of (Vp) at the selected position and Roman numerals indicate relevant LVZs.

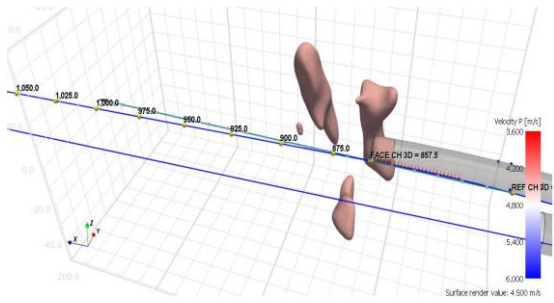


Figure 11 3D view of Vp with a surface rendering that appears to contain low speed zones (render value Vp=4,500 m/s). The value of the rendering was set a little higher to delimit areas with lower Vp value from the reference as far as possible.

5.1.2. S- Wave Velocity Model:

Figure 12, 2D longitudinal and plan sections (top and bottom, respectively) which were extracted from the 3D model of the SV-wave velocity on the seismic axis. Similar as in the Vp distribution model, Vs distribution is also dominated by lower velocity values.

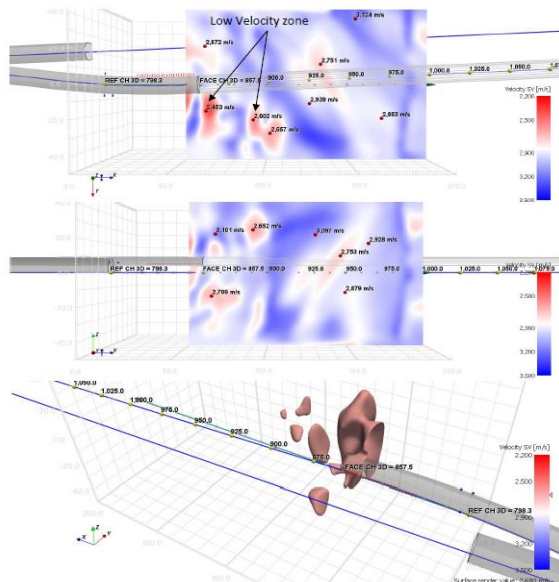


Figure 12 Top & Longitudinal view of the 3D SV wave velocity model along the tunnel axis including the tunnel model with the location of the shot holes (red dots) and the receivers (blue dots). The comparatively low velocities zones are indicated by black arrows and Roman numerals indicate relevant LVZs. The bottom part shows surface rendering that appears to contain lower velocity zones (render value =2,650m/s).

At an approximate RD 930, another drop in Vs is measured, which is slightly below the reference value. The low velocity zones in S wave may be associated with a detriment of the rock condition and with possible wet to minor water bearing zones.

5.1.3. P wave Migration:

The process of migration maps seismic amplitude that are recorded as function of time to model space utilizing travel time of waves propagating through the velocity model. Results coming from the 3D processing are represented by two main outputs, RMS amplitude, and (P)&(S)-wave velocity distributions. The RMS amplitude distribution quantifies the level of reflectivity throughout the modelled area. Large RMS values with positive or negative signs, correspond to areas of high “illumination”. In other words, the areas from where the most reflections obtained through 3D processing. This is an output from the so-called seismic migration process. The reflective zones can be associated to boundaries, where significant changes in the rock condition might be expected. Highest negative values (dark blue) are found at rz1. Negative values are associated to changes from higher to low velocity while red values to the contrary in figure - 13.

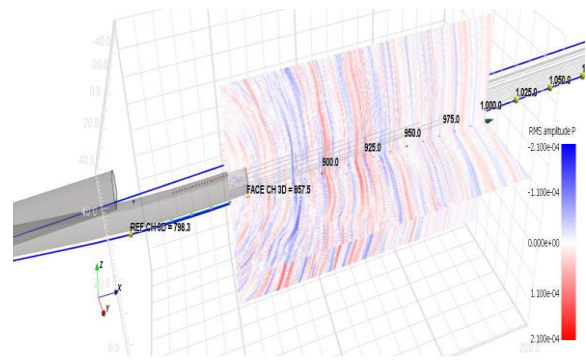


Figure 13- Plan & longitudinal View extracted from the 3D RMS amplitude image for P –wave. High reflectivity zones are shown by black arrow mark.

5.1.2. Prognosis along tunnel axis :

The core of the interpretation based on TSP results depends on contradiction between reference values, i.e., the estimated seismic velocities within the TSP layout and geo-mechanical parameters and values of these parameters associated with the extracted reflectors along the estimated boundary. Furthermore, geological observations with the TSP layout and

existing geological models allow preliminary correlation of these values. Keeping these aspects in mind, the forecast for this campaign is as follows:

Table -8

Parameter	#4_RD 857_ P1 downline
Vp (m / s)	4,936
Vs (m / s)	2,853
Poisson ratio (-)	0.25
Edyn (GPa)	54
Stat Edyn (GPa)	38
Geology	Weak to mod strong rock mass - Phyllitic Quartzite.

a) RD 857 to RD 867

Parameter	Vp [m / s]	Vs [m / s]	Poisson	Edyn [GPa]	Stat Edyn [GPa]
values	4,876	2,837	0.24	53	36
tendency	Slight decrease	comparable	Slight decrease	comparable	Slight decrease
Interpretation	Slight decrease in rock stiffness.				
Remarks					

b) RD 867 to RD 882

Parameter	Vp [m / s]	Vs [m / s]	Poisson	Edyn [GPa]	Stat Edyn [GPa]
values	4,148 - 4,431	2,494 - 2,698	0.19 - 0.22	37 - 45	21 - 28
tendency	Decreasing	Decreasing	Slight decrease	Decreasing	Decreasing
Interpretation	Decrease in rock stiffness.				
Remarks	More drop in Vp & Vs is found towards right tunnel wall side, which might be associated with some shear zone/increase in rock mass fracturing				

c) RD 882 to RD 893

Parameter	Vp [m / s]	Vs [m / s]	Poisson	Edyn [GPa]	Stat Edyn [GPa]
values	4,669	3,013	0.14	56	39
tendency	Increasing	Increasing	decreasing	Increasing	Increasing
Interpretation	Comparatively improvement in rock mass stiffness				
Remarks					

d) RD 893 to RD 907

Parameter	Vp [m / s]	Vs [m / s]	Poisson	Edyn [GPa]	Stat Edyn [GPa]
values	4,901 - 5,419	2,978 - 3,041	0.21 - 0.14	60 - 63	44 - 47
tendency	Increasing	Increasing	Increasing	Increasing	Increasing
Interpretation	Increase in rock mass stiffness				
Remarks					

e) RD 907 to RD 913

Parameter	Vp [m / s]	Vs [m / s]	Poisson	Edyn [GPa]	Stat Edyn [GPa]
values	4,728	2,971	0.17	56	39
tendency	Decreasing	Slight decrease	decreasing	decreasing	decreasing
Interpretation	Slight decrease in rock stiffness /possible increase of fracturing				
Remarks	A low velocity zone is found away from tunnel axis (~20-25m from axis, towards right wall, where Vp reduced to 4,229m/s. This may cut the tunnel axis approximately at RD907. This zone can be interpreted as possible increase of rock fracturing/jointing or some shear zone.				

g) RD 927 to RD 939

Parameter	Vp [m / s]	Vs [m / s]	Poisson	Edyn [GPa]	Stat Edyn [GPa]
values	4,870	3,038	0.18	59	43
tendency	Slight decrease	comparable	comparable	Slight decrease	Slight decrease
Interpretation	Comparatively slight decrease in rock stiffness.				
Remarks	A comparatively low velocity zone is found in vertical component of S wave, approximately at RD930 (~7 -10m thick). This zone can be interpreted as possible water bearing zone/increase of fracturing/jointing.				

h) RD 939 to RD 958

Parameter	Vp [m / s]	Vs [m / s]	Poisson	Edyn [GPa]	Stat Edyn [GPa]
values	5,190	3,016	0.25	62	47
tendency	Increasing	comparable	Increasing	Increasing	Increasing
Interpretation	Increase in rock mass stiffness.				
Remarks					

i) RD 958 to RD 966

Parameter	Vp [m / s]	Vs [m / s]	Poisson	Edyn [GPa]	Stat Edyn [GPa]
values	5,065	2,863	0.27 - 0.28	56	39
tendency	Slight decrease	decreasing	Increasing	decreasing	decreasing
Interpretation	Slight deterioration in rock mass stiffness might be expected.				
Remarks	Possibility of water bearing zone can not be disregarded.				

j) RD 966 to RD 996

Parameter	Vp [m / s]	Vs [m / s]	Poisson	Edyn [GPa]	Stat Edyn [GPa]
values	5,252 - 5,283	2,881 - 2,983	0.23 - 0.28	58 - 60	42 - 44
tendency	Increasing	Slight increase	Comparable to prev.	decreasing	decreasing
Interpretation	Increase in rock stiffness.				
Remarks					

CONCLUSION

In this study, the application of Modern Tunnel Seismic Prediction (TSP) techniques provided important insights into the condition of rock mass ahead of the tunnel faces for both the U/P (Main Tunnel - M/T) line and the D/N line tunnel, for the U/P line tunnel the rock mass is predicted to extend up to 110 meters beyond the tunnel face. The velocity distributions indicate that the entire predicted area generally exhibited similar rock mass conditions with some local variations in velocity. However, two lower velocity zones were identified near the tunnel axis at approximately Ch48+229.00m and Ch48+257.00m. For the D/N line tunnel, the rock mass prediction extends up to 109 meters beyond the tunnel face. Similar to the U/P line, the entire predicted area displayed approximately uniform rock mass positions with some local improvements in velocity. Two lower

velocity zones were anticipated directly ahead of the tunnel face, from RD867.00m to RD883.00m and RD907.00m to RD913.00m, suggesting potential decreases in rock mass stiffness or increases in rock mass fracturing. The first zone showed a more significant drop in velocity compared to the second zone. Additionally, a slight drop in S-wave velocity was detected around RD930, indicating a potential wet to minor water-bearing zone with an increased likelihood of fracturing or jointing in the rock mass.

The successful launch of the TBMs demonstrated the efficacy of using TSP technology for advance prediction and preparation in complex geological conditions. The TSP results were verified through probe holes and Measurement While Drilling (MWD) data during TBM operational after 20 m from the lanching tunnel faces. The study recommends the continued use of TSP and ISP (Mechanical Hammer Process Campaigns) as integral components of TBM tunnelling operations, particularly for challenging projects like the RVNL Package-4 of the New BG Rail Line Project in Rishikesh, Uttarakhand, India.

REFERENCE

- [1] Amberg TSP Ease Processing version 2.1.10569 (64 bit), TSP 303 Plus
- [2] Hook & Brown rock mechanics book, Geotech TSP 203: Case Histories, Amberg, Delhi, India, Tunnel seismic prediction and its applications, INDOROCK-20167-3D TSP- Advanced geological prediction,
- [3] Paper ISRM_2011 Dickmann & Pittard, Paper WTC-2013 Dickmann & ruger.
- [4] Paper WTC-2010 Dickmann & Groschup ,Peper Tunconstruct 2009 Dickmann & Groschup.
- [5] TSP-303 brochure-2017, JRMTT-2014 Dickmann, Paper -Geomechanik & tunnelbau 2008 _ Dickmann.
- [6] Smith, J. (2020). "Seismic Prediction Methods for Tunnel Boring: A Comparative Study." *Journal of Geotechnical and Geoenvironmental Engineering*, 146(3), 123-137.
- [7] Doe, J. (2018). "Innovations in Tunnel Boring Machine Technology and Geotechnical Analysis." *Tunnelling and Underground Space Technology*, 73, 45-59.
- [8] Johnson, E. (2019). "Application of Geophysical Techniques in Tunnel Construction: Case Studies." *Journal of Applied Geophysics*, 167, 104-118.
- [9] Brown, M. (2021). "Advances in Rock Mass Characterization for Tunnelling in Complex Geologies." *Engineering Geology*, 282, 105-117.
- [10] Lee, S. (2022). "Integrating TSP and NATM for Efficient Tunnel Construction in Mountainous." *Journal of Applied Geophysics*, 167, 104-118.
- [11] Green, R. (2023). "Geomechanical Properties and Seismic Prediction in Tunnel Boring." *Journal of Applied Geophysics*, 167, 104-118.
- [12] Garcia, M. (2021). "Tunnelling Through the Himalayas: Challenges and Technological Solutions." *Journal of Mountain Science*, 18(2), 201-215.
- [13] White, R. (2019). "Hydrogeological Implications in Tunnel Seismic Prediction." *Journal of Hydrology*, 574, 673-685.
- [14] Kim, L. (2020). "Comparative Analysis of TSP and MWD Methods in Tunnel Boring." *Geotechnical and Geological Engineering*, 38(4), 299-312.
- [15] Harris, W. (2022). "Rock Mass Quality Assessment Using Seismic Velocities in Tunnel Engineering." *Journal of Applied Geophysics*, 167, 104-118.